Alternatively spliced isoforms of WT1 control podocyte-specific gene expression

Jonathan Lefebvre[1,2,3,11], Michael Clarkson[1,2,3,11], Filippo Massa[1,2,3,11], Stephen T. Bradford[1,2,3,4,5], Aurelie Charlet[1,2,3], Fabian Buske[4,5], Sandra Lacas-Gervais[6], Herbert Schulz[7,12], Charlotte Gimpel[8], Yutaka Hata[9], Franz Schaefer[10] and Andreas Schedl[1,2,3]

[1]Institute of Biology Valrose, Université de Nice-Sophia, Nice, France; [2]Inserm, UMR1091, Nice, France; [3]CNRS, UMR7277, Nice, France; [4]CSIRO Food and Nutrition Flagship, North Ryde, New South Wales, Australia; [5]Epigenetics Group, Cancer Program, Garvan Institute of Medical Research, Darlinghurst, New South Wales, Australia; [6]CCMA University of Nice, Nice, France; [7]MDC for Molecular Medicine, Berlin, Germany; [8]University Children's Hospital, Freiburg, Germany; [9]Tokyo Medical and Dental University, Tokyo, Japan and [10]University Children's Hospital, Heidelberg, Germany

The Wilms' tumor suppressor WT1 is a key regulator of podocyte function that is mutated in Denys–Drash and Frasier syndromes. Here we have used an integrative approach employing ChIP, exon array, and genetic analyses in mice to address general and isoform-specific functions of WT1 in podocyte differentiation. Analysis of ChIP-Seq data showed that almost half of the podocyte-specific genes are direct targets of WT1. Bioinformatic analysis further identified coactivator FOXC1-binding sites in proximity to WT1-bound regions, thus supporting coordinated action of these transcription factors in regulating podocyte-specific genes. Transcriptional profiling of mice lacking the WT1 alternative splice isoform (+KTS) had a more restrictive set of genes whose expression depends on these alternatively spliced isoforms. One of these genes encodes the membrane-associated guanylate kinase MAGI2, a protein that localizes to the base of the slit diaphragm. Using functional analysis in mice, we further show that MAGI2α is essential for proper localization of nephrin and the assembly of the slit diaphragm complex. Finally, a dramatic reduction of MAGI2 was found in an LPS mouse model of glomerular injury and in genetic cases of human disease. Thus, our study highlights the central role of WT1 in podocyte differentiation, identifies that WT1 has a central role in podocyte differentiation, and identifies MAGI2α as the crucial isoform in slit diaphragm assembly, suggesting a causative role of this gene in the etiology of glomerular disorders.

Kidney International (2015) **88,** 321–331; doi:10.1038/ki.2015.140; published online 20 May 2015

KEYWORDS: glomerular disease; kidney development; nephrin; podocyte differentiation; slit diaphragm; WT1

Correspondence: *Andreas Schedl, Inserm UMR1091, Centre de Biochimie, Parc Valrose, 06108 Nice, France. E-mail: Schedl@unice.fr*

[11]These authors contributed equally to this work.

[12]Current address: Cologne Center for Genomics (CCG), Cologne, Germany

Received 6 September 2014; revised 26 March 2015; accepted 26 March 2015; published online 20 May 2015

Glomerular podocytes are highly specialized cells with unique cellular extensions (foot processes) that interact via integrin with the basement membrane. Actual filtration takes place at the slit diaphragm, a multiprotein complex that connects adjacent podocytes via pairing of nephrin molecules that are anchored in the cell membrane of two opposing foot processes. Nephrin interacts with a multitude of proteins including podocin, NCk, and CD2AP.[1] Moreover, mass spectrometry has identified a set of additional interaction partners including IQGAP, MAGI2, and CASK that are believed to connect the slit diaphragm to the actin cytoskeleton.[2] IQGAP has also been shown to be required for podocyte migration.[3]

The Wilms' tumor suppressor WT1 encodes a zinc-finger protein that serves key functions in kidney development.[4] WT1 encodes up to 36 protein variants that are produced by a combination of alternative splicing, alternative translation start sites, and RNA editing. Of particular importance appears to be alternative splicing within the zinc-finger region that results in the inclusion (WT1(+KTS)) or omission (WT1(−KTS)) of the three amino acids KTS. Molecular and cellular data indicate distinct functions for these isoforms: although WT1(−KTS) variants are considered as transcriptional regulators, WT1(+KTS) isoforms have a stronger affinity to RNA and have been suggested to be involved in splicing.[5,6] A confirmation or refutation of this hypothesis *in vivo* is, however, missing.

WT1 function is crucial in podocyte maintenance, and mutations in this gene have been found in patients suffering from glomerular diseases including Denys–Drash syndrome[7] and Frasier syndrome.[8,9] Both of these syndromes are characterized by the development of glomerular sclerosis, but the molecular mutations found in WT1 are distinct: whereas Denys–Drash patients usually carry missense or nonsense mutations within the zinc-finger region that lead to a protein that can no longer bind to DNA,[10] mutations in Frasier patients disrupt the alternative splice donor site in intron 9, thus interfering with WT1(+KTS) isoform

production.[8,9] As Frasier mutations are heterozygous, the syndrome appears to be caused by an imbalance of +KTS and −KTS isoforms.

Our laboratory has previously generated mouse lines that specifically interfere with the production of WT1(+KTS) or WT1(−KTS) isoforms.[11] Heterozygous mutations that interrupt WT1(+KTS) production ($Wt1(+KTS)^{+/-}$) develop glomerular sclerosis and thus represent a mouse model for the Frasier syndrome. Homozygous mutations ($Wt1(+KTS)^{-/-}$) show a more severe phenotype and fail to form foot processes.[11] Mice homozygous for the *Wt1(−KTS)* mutation are even more severely affected, and differentiated glomerular structures were rarely visible. The molecular events underlying the phenotypes in *Wt1(+KTS)* and *Wt1(−KTS)* mutants remain, however, elusive.

Here we have analyzed the podocyte-specific function of WT1 using a range of tools and show that WT1 is directly regulating a large proportion of podocyte-specific genes. Using microarray analysis on WT1(+KTS) mutant glomeruli, we further show that this isoform is required for the expression of a subset of podocyte-specific genes. Finally, we performed functional analysis of one of these genes, *Magi2*, and show that it is an essential component of the slit diaphragm complex that is required for nephrin localization and foot process formation.

RESULTS

Wt1 is a central transcriptional regulator of podocyte-specific genes

To evaluate the degree of glomerular development in mice lacking alternatively spliced isoforms of WT1,[11] we performed immunofluorescent analysis on E18.5 kidney sections. As previously reported, nephrin (NPHS1) was absent from *Wt1(−KTS)* kidneys (Supplementary Figure S1 online),[12] and also podocyte-specific proteins such as podocin (NPHS2) and the actin-associated protein Synaptopodin (SYNPO) were lacking or severely reduced, thus confirming an absolute requirement of this isoform for podocyte differentiation (Supplementary Figure S1 online). In contrast, immunofluorescence analysis of *Wt1(+KTS)* knockout animals showed the presence of all three markers. Careful examination of high-power views revealed a somewhat less complex staining, consistent with a less developed glomerular tuft. In addition, nephrin staining was punctuated in $Wt1(+KTS)^{-/-}$podocytes, a pattern that was in stark contrast to the continuous line of staining along the basement membrane in control sections (Supplementary Figure S1 online).

We have previously performed chromatin immunoprecipitation-sequencing (ChIP-Seq) analysis on E17.5 kidneys to identify genome-wide targets for WT1.[13] To identify glomerular-specific genes potentially regulated by WT1, we examined the overlap between the ChIP-associated genes (irreproducible discovery rate (IDR) <0.1) with gene lists that represent the Top200 genes specifically expressed in glomerular cell types.[14] Although gene lists of endothelial (Tie2-sorted) and juxta-glomerular cells (Ren1-sorted) showed no significant overlap, 91 genes out of 192 podocyte-specific genes (MafB-sorted) were associated with WT1-bound regions (IDR $\leqslant 0.1$) (Figure 1a and Supplementary Data S1 online). This strong association persisted even when using the more stringent cutoff of IDR $\leqslant 0.01$ (64/192 genes; Figure 1b and Supplementary Data S1 online). Interestingly, *WT1* seems to regulate several members of the integrin (*Itga3*, *Itgav*, *Itgb5*, *Itgb8*) and myosin gene families (*Myo1d*, *Myo1e*, *Myo6*) that are important for the interaction with the basement membrane and intracellular movement, respectively. In addition, the crucial genes, *MafB*,[15] *Nphs1*,[16] and *Nphs2*,[17] showed strong WT1-associated peaks (Figure 1c).

MEME (Multiple EM for Motif Elicitation) analysis performed on the 91 sequences bound by WT1 (IDR $\leqslant 0.01$; within 2.5 kb of a podocyte-specific gene) identified a motif highly similar to the previously characterized WT1-binding sequence,[13] indicating that podocytes use canonical WT1 binding (Figure 1d). Motif enrichment analysis[18] revealed the presence of FOX (for example, FOXC1; $P = 4.85e-12$) transcription factor–binding motifs, suggesting concerted action of these proteins in the regulation of podocyte-specific genes (Figure 1e and Supplementary Figure S2 online). In addition, binding sites for helix-loop-helix transcription factors were found to be enriched (for example, NHLH1; $P = 2.71e-10$).

Microarray analysis reveals a set of deregulated genes in Wt1 (+KTS) mutant mice

Frasier syndrome is caused by a reduction of Wt1(+KTS) isoforms, but the molecular events leading to this glomerular disease are unknown. To identify potential targets for these isoforms, we performed microarray analysis on isolated glomeruli from E18.5 wild-type and Wt1(+KTS) knockout animals. Because WT1(+KTS) has been suggested to have a role in RNA splicing, we opted for exon arrays that are designed to detect alternatively spliced isoforms (Figure 2a and Supplementary Figure S3A online). As expected, overall *Wt1* expression was unchanged, implying increased expression of WT1(−KTS) variants in these animals (Supplementary Figure S3B online). Analysis of the microarray data on the exon level (Supplementary Data S2, worksheet 1, online) followed by quantitative real-time PCR assays (data not shown) did not identify significant differences in exon usage in mutant mice, and we therefore subsequently focused on changes in overall gene expression levels (Supplementary Data S2, worksheet 3, online).

We performed gene enrichment analysis using ranked gene lists and the GOrilla toolset (http://cbl-gorilla.cs.technion.ac.il/).[19] Genes induced in *Wt1(+KTS)* mutant glomeruli showed a significant enrichment of chemokine activity (388-fold; $P = 3.3e-08$), when analyzed for FUNCTION, and immune response (fourfold; $P = 7.7e-10$) and neuron projection guidance (fourfold; $P = 2.3e-6$), when analyzed for PROCESS (Supplementary Data S3 online). The same analysis performed for genes with reduced expression

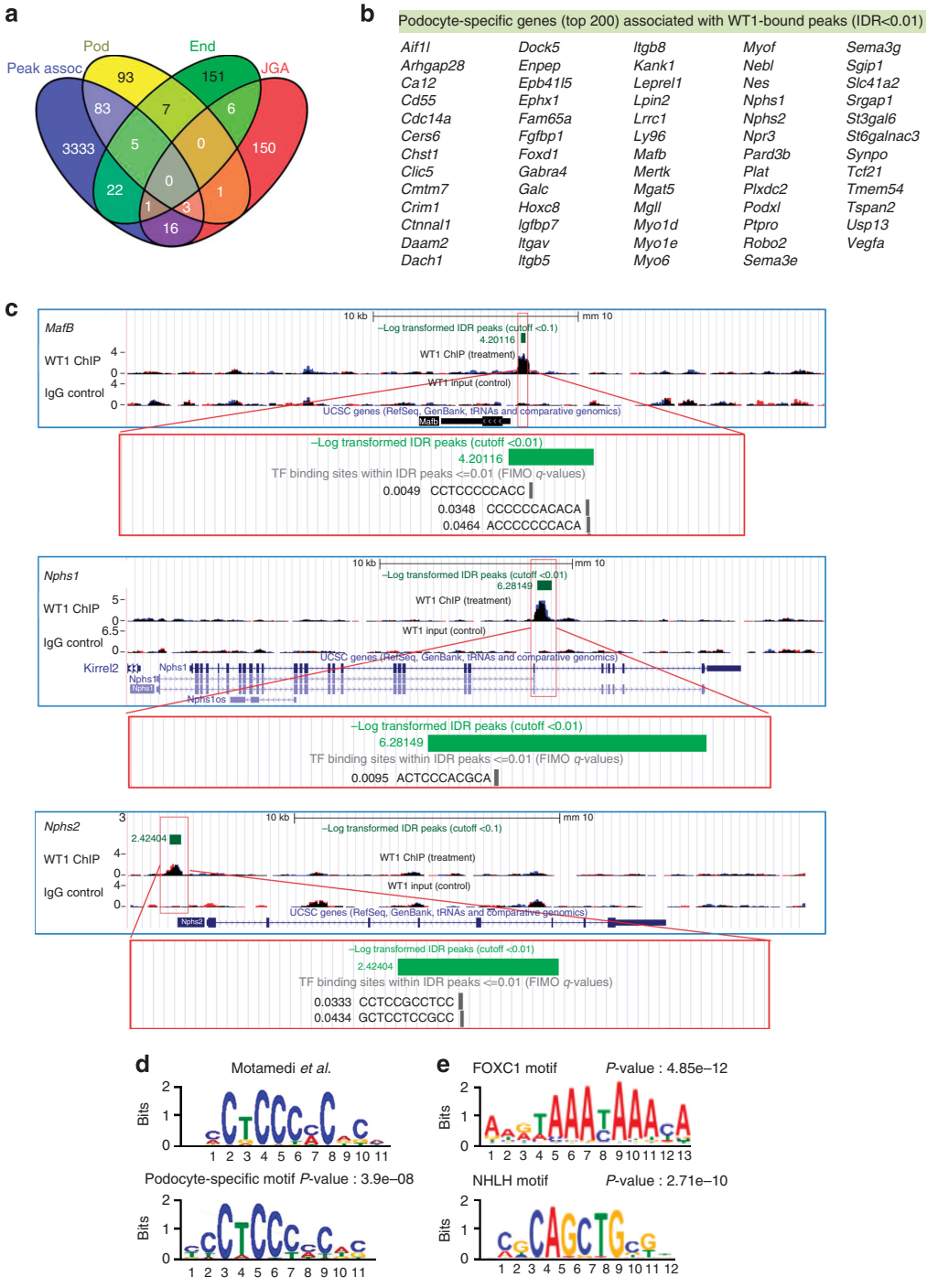

Figure 1 | WT1 regulates a large proportion of podocyte-specific genes. (**a**) Venn diagram showing overlap between genes with WT1-bound peaks (blue) and genes specific for podocytes (Pod; yellow), endothelial cells (End; green), and juxtaglomerular apparatus (JGA; red). Cell type–specific gene lists (Top200 genes) were obtained from the GUDMAP database (www.gudmap.org). (**b**) Alphabetic gene list showing the 64 podocyte-specific genes with WT1-bound peaks (irreproducible discovery rate (IDR) <0.01). (**c**) Peak visualization for three representative genes with important function in podocyte development. Tracks were generated by overlaying two independent WT1 chromatin immunoprecipitation-sequencing (ChIP-Seq) data sets (WT1-ChIP-Seq data are represented in red and blue, regions with overlap are depicted in black). Log-transformed peaks *Mafb* (IDR = 6.29e –05), *Nphs1* (IDR = 5.23e – 07), and *Nphs2* (IDR = 0.0037) are given in green above the tracks. The inserts show in detail the presence of WT1-binding consensus sequences (FIMO) with significant *q*-value score. (**d**) Motif discovery in the 91 WT1-bound regions on podocyte-specific genes (GUDMAP; Mafb200 genes list) revealed a motif almost identical to the previously published WT1-binding site.[13] (**e**) Bioinformatic analysis (AME algorithm, version 4.10.0) identified enrichment for consensus sequences of FOXC1 (*P*-value = 4.85e – 12) and helix-loop-helix TFs (NHLH1; *P*-value = 2.71e – 10). IgG, immunoglobulin G; TF, transcription factor.

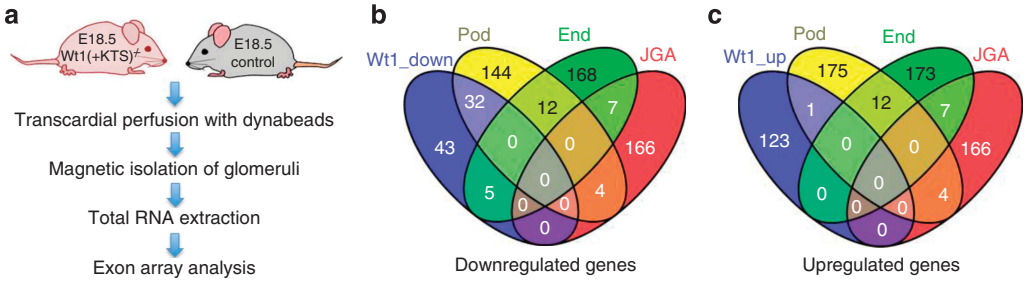

d

Gene name	Array fold change Fras vs WT (*P*-value)	qRT-PCR fold change Fras vs WT (*P*-value)	KO kidney phenotype	Reference
Cd59b	–4.37 (3.85E-05)	ND	No KO	
Cd59a	–3.80 (2.82E-06)	–1.91 (2.96E-05)	Not reported	(43)
Tdrd5	–3.71 (6.79E-06)	–5.41 (1.32E-01)	Not reported	(44)
Nell2	–3.59 (3.72E-06)	–9.95 (1.74E-04)	Not reported	(45)
Thsd7a	–3.54 (2.58E-05)	–5.61 (1.08E-04)	No KO	
C1qtnf1	–3.12 (2.58E-04)	–5.02 (2.31E-04)	No KO	
Sgip	–3.02 (4.98E-07)	–7.65 (1.19E-05)	No KO	
Sema3e	–2.82 (2.88E-07)	ND	Not reported	(46)
Rab3b	–2.81 (4.13E-06)	–7.65 (1.47E-05)	Not reported	(47)
Clic3	–2.75 (1.01E-04)	–10.82 (8.19E-05)	No KO	
Sla	–2.62 (1.72E-05)	–8.34 (4.51E-05)	Not reported	(48)
Col4a3	–2.61 (5.78E-06)	–4.76 (4.43E-05)	Alport syndrome	(49)
Nphs2	–2.43 (1.73E-04)	–3.89 (6.64E-04)	FSGS	(50)
Ptpro	–2.42 (1.22E-05)	–5.47 (6.59E-06)	Low GFR	(51)
Ehd3	–2.39 (7.34E-05)	ND	Proteinuria in Ehd3$^{-/-}$ Ehd4$^{-/-}$	(52)
Top1mt	–2.38 (1.93E-04)	ND	Not reported	(53)
Asb15	–2.34 (2.65E-04)	ND	No KO	
Htra1	–2.32 (1.87E-04)	ND	Not reported	(54)
Nebl	–2.29 (9.11E-06)	–2.80 (6.78E-05)	No KO	
Sema3g	–2.22 (1.20E-04)	ND	No KO	
Ggt5	–2.21 (2.81E-05)	ND	Not reported	(55)
Magi2	–2.15 (8.01E-05)	–5.18 (1.66E-04)	FSGS	(25,26)
H6pd	–2.06 (1.51E-05)	ND	Not reported	(56)
Cd55	–2.05 (1.38E-05)	ND	Not reported	(57)

Figure 2 | Transcriptional profiling of glomeruli in *Wt1(+KTS)*$^{-/-}$ (Frasier) mice reveals changes of a subset of podocyte-specific genes. (**a**) Schematic representation of the procedure used for exon array analysis. (**b**, **c**) Venn diagram showing the overlap between (**b**) 90 downregulated genes or (**c**) 124 upregulated genes in *Wt1(+KTS)* mutants presenting a fold change higher than 1.5 (Wt1_down; blue) and compared with podocyte-specific genes ('Pod', in yellow), endothelial cells (End; green), and juxtaglomerular apparatus (JGA; red). The gene lists used were obtained from GUDMAP data set bank. (**d**) List of the top genes dowregulated in *Wt1(+KTS)* mutants, ordered by decreasing fold change compared with the wild type (WT). The data were validated by quantitative real-time reverse transcription–PCR (qRT-PCR; $n > 4$), and the related kidney phenotypes in mouse models are referred to in the last column. FSGS, focal segmental glomerulosclerosis; GFR, glomerular filtration rate; KO, knockout; ND, not determined.

revealed only minor enrichment (response to toxic substances fourfold; $P = 1.7e-6$).

Statistical analysis (false discovery rate $< 5e-2$) identified 80 (38) probe sets with >1.5-fold (>2-fold) reduction in gene expression and 96 (35) probe sets with >1.5-fold (>2-fold) increase in gene expression. Comparison with cell type–specific gene lists (GUDMAP) showed a marked enrichment of podocyte-specific genes in the downregulated

genes and 40% of genes with >1.5-fold change figured in the Top200 podocyte-specific gene list (Figure 2b and Supplementary Data S2 online). Further analysis of genes with more than twofold decrease using the GUDMAP database confirmed the presence of podocyte-specific genes (Figure 2d and Supplementary Figure S4 online). No such enrichment was found for genes showing >1.5-fold increased expression (Figure 2c).

In all, 12 out of the 38 genes downregulated (>2-fold) showed WT1-bound peaks in proximity to their respective transcription start site (Supplementary Figure S4 online, right column), including the known podocyte-specific gene *Nphs2* (Figure 1c). In contrast, only 3 genes (*Itga11*, *Nipal2*, and *Krt19*) with induced expression (>2-fold) showed peaks in their proximity, suggesting that the main function of WT1 (+KTS) in podocytes is to induce rather than to repress gene expression.

WT1 directly binds to the Magi2α promoter

Several of the genes that showed reduced expression in Wt1 (+KTS) knockout mice are interesting candidates for genes involved in glomerular damage. For some of these, knockout animals have been generated (Figure 2d), and although a detailed analysis on kidneys has not been performed in all cases, survival of mutants suggests that these genes do not have a predominant role in foot process formation. We concentrated on *Magi2* [20] for multiple reasons. First, MAGI2 has been shown to be expressed in glomerular podocytes.[2,21] Second, it can interact with nephrin at a molecular level.[2] Third, MAGI2 has been shown to be involved in neuronal spine formation,[22] a process that involves cytoskeletal rearrangements.

MAGI2 exists in several isoforms that are produced by the use of alternative translation start sites.[23] Examination of ChIP-Seq data revealed two peaks in the promoter region of *Magi2*α (IDR <0.1), but not *Magi2*β or *Magi2*γ promoters (Figure 3a). Closer inspection of peak sequences using FIMO (Find Individual Motif Occurrences) predicted several WT1-binding sites. To confirm direct binding of WT1 to this region, we carried out ChIP-PCR experiments using independent ChIP samples and two different antibodies. WT1-precipitated material was fourfold and ninefold enriched over immunoglobulin G control samples for regions I and II, respectively. No such enrichment was found with primers mapping 38 kb downstream of the promoter start site (Figure 3b). Finally, transfection studies in U2OS cells with reporter constructs containing sites I and II demonstrated specific action of WT1 on the *Magi2*α promoter (Supplementary Figure S5 online). However, in this cell system, WT1 repressed, rather than activated, the promoter, suggesting the absence of podocyte-specific coactivators (such as FOXC1) or the presence of corepressors in these cells. A cell type–dependent suppression or activation of promoters by WT1 has been reported previously in other systems.[24]

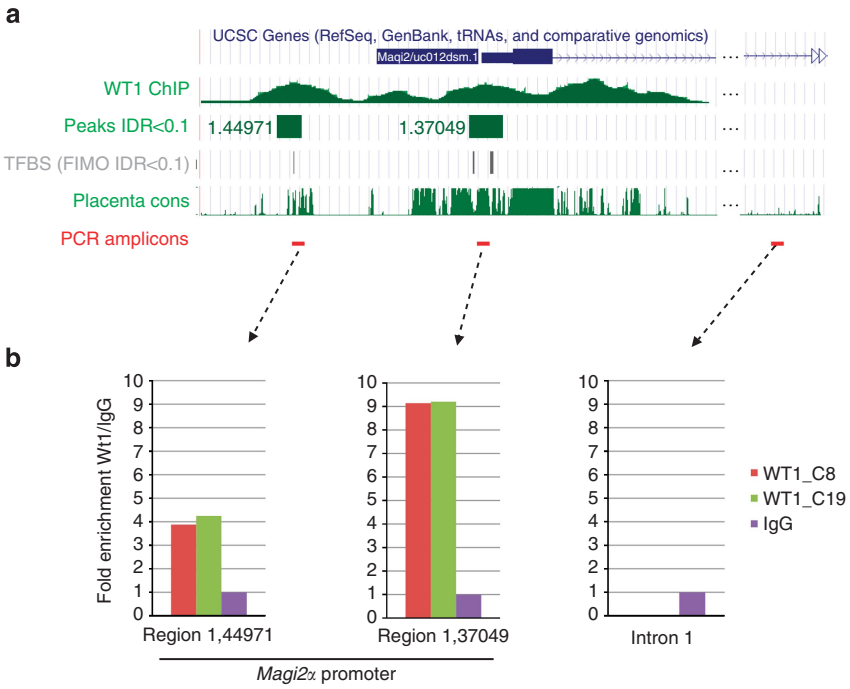

Figure 3 | Chromatin immunoprecipitation-sequencing (ChIP-Seq) and ChIP-PCR reveal direct binding of WT1 to the *Magi2*α promoter. (**a**) Visualization of ChIP-Seq data reveals binding of WT1 to the *Magi2*α promoter (irreproducible discovery rates (IDRs) = 0.043; 0.036). Tracks were generated from two independent WT1-ChIP-Seq data sets. WT1-binding regions as predicted by FIMO, as well as evolutionary conservation in placental animals, are shown below the track. (**b**) Quantitative real-time PCR (QPCR) validation of WT1-binding regions. ChIP was performed on isolated glomeruli from adult mice using two independent antibodies against WT1 (C19, C8). QPCR analysis with specific primers shows enrichment for the two peaks within the promoter, but not a region mapping 38 kb downstream of the *Magi2*α start site. TFBS, transcription factor-binding sites.

Magi2α is the crucial isoform in podocyte differentiation

Two recent studies using distinct knockout alleles have shown *Magi2* to be required for podocyte function, but with somewhat different results. Although mice truncated after exon 5 showed a complete absence of the slit diaphragm,[25] deletion of exon 4 resulted in progressive glomerular disease.[26] To clarify this discrepancy and to test which isoform of *Magi2* may be essential for podocyte differentiation, we analyzed kidneys from a third *Magi2* knockout model[22] that lacks exon 1 (*Magi2*α), but should maintain the expression of *Magi2*β and *Magi2*γ isoforms. Quantitative real-time PCR analysis on RNA isolated from E18.5 and P0 kidneys using primers designed to detect all three isoforms of *Magi2* showed a complete absence of *Magi2* transcripts, confirming that *Magi2*α is the predominant isoform produced in glomerular podocytes (Supplementary Figure S6 online).

Macroscopic inspection of kidneys from *Magi2*α knockout mice revealed no difference in renal size, but bladders of mutant neonates were empty, suggesting lack of urine production. Histological analysis showed an overall normal glomerular architecture (Supplementary Figure S7A online). Scanning electron microscopy of knockout kidneys revealed the presence of primary and secondary processes, but the absence of the sophisticated interdigitation of foot process seen in wild-type podocytes (Figure 4a, I and IV). Instead, mutant podocytes displayed poorly organized extension reminiscent of filipodia. Endothelial cells appeared normal, showing the typical fenestration (Supplementary Figure S8 online). Transmission electron microscopy confirmed defects in cytoskeletal organization in *Magi2*α knockout podocytes, and slit diaphragms were missing (Figure 4a, II and V, and Supplementary Figure S8 online). Thus, deletion of *Magi2*α results in a phenotype comparable to that reported by Ihara *et al.*,[25] suggesting that the less severe phenotype in Balbas *et al.*[26] is a hypomorph (see discussion).

Expression analysis confirmed the persistence of podocyte-specific genes such as *WT1*, *Nphs1*, *Nphs2*, *Podx*, *Synpo*, and *CD2AP* (Supplementary Figure S7B and C online). Interestingly, although protein expression levels of nephrin remained unchanged, as judged by western blot analysis (Figure 4c), detection by immunohistological methods was severely hampered (Figure 4d). Prolonged exposure time revealed a weak speckled nephrin signal, suggesting altered cellular localization of this protein (Figure 4e, most right panels). Immunogold labeling further confirmed the marked reduction of nephrin signal in *Magi2*α mutant podocytes. In rare occasions, when a signal was detected, it localized intracellularly (Figure 4a, III and VI). We conclude that MAGI2 is required for proper localization of nephrin within foot processes and thus the assembly of the slit diaphragm.

Loss of *MAGI2* expression correlates with glomerular diseases in mice and humans

To test whether *Magi2* expression was disrupted in other circumstances in which podocyte foot process effacement is observed, we treated mice with lipopolysaccharide (LPS) that results in transient proteinuria and disruption of foot processes.[27] RNA analysis on isolated glomeruli revealed an initial sevenfold reduction of *Magi2* expression that coincided with podocyte injury (Figure 5a). *Magi2* expression returned to normal levels upon recovery of kidney function.

To investigate whether a similar link can be found in human disease, we made use of the data available in the Nephromine database, a resource of microarray expression data from microdissected renal biopsies. Strikingly, *MAGI2* featured in the top genes deregulated in glomerular disease in all microarray sets analyzed, with a 3.2-fold ($P = 0.005$) change in focal segmental glomerulosclerosis and as much as 6.2-fold change ($P = 6.13e-7$) in diabetic nephropathy (Figure 5 and Supplementary Figure S9 online). We further compared *MAGI2* transcript levels in disease databases with the expression of other genes that are known to be required for podocyte function and/or are associated with podocyte disease. Of the selected genes, *MAGI2* was the most highly downregulated gene in focal segmental glomerulosclerosis (Hodgin, −3.28-fold, $P = 0.005$), IgA nephropathy (Reich, −1.54-fold, $P = 2.29e-7$; Ju, −1.47-fold, $P = 6.05e-5$), and Lupus (Berthier, −2.07-fold, $P = 1.56E-8$; Ju, −1.73-fold, $P = 4.9E-6$), and the second most highly downregulated gene in diabetic nephropathy (Woroniecka, −6.2 = fold, $P = 6.13E-7$) (Supplementary Figure S9 online).

Finally, we analyzed a panel of biopsies from patients suffering from glomerular diseases for potential changes in MAGI2 expression (Figure 5f–i). Despite the persistence of the podocyte-specific marker synaptopodin, MAGI2 signal was markedly reduced in several samples including cases of membranoproliferative glomerulonephritis and genetic cases of focal segmental glomerulosclerosis (*Cox2* and *Nphs2* mutations).

DISCUSSION

Podocytes are highly specialized cells that express a unique combination of proteins required to build the intricate structure of the slit diaphragm. Differentiation requires a network of transcription factors, and WT1 clearly holds a key role in this process. Indeed, several podocyte-specific WT1 targets have been reported previously, including *Nphs1*,[12,28] *Neph3*,[29] *Sulf1*,[30,31] and *Scel*.[31] The analysis presented here demonstrates that WT1 regulates a much broader set of genes, and almost 50% of the top 200 podocyte-specific genes—as defined in the GUDMAP gene expression atlas[14]—were bound by WT1 (IDR $\leqslant 0.1$). Given this central role, it is not surprising that upregulation of miR-193a, a repressor of WT, causes focal segmental glomerulosclerosis in human patients.[32]

Although WT1(−KTS) knockout mice demonstrate an essential role for WT1 in regulating podocyte genes, it clearly requires cofactors. Studies in zebrafish have recently suggested interaction with FOXC1 and RBPJ in driving podocyte differentiation.[33] The bioinformatic analysis presented here confirms the presence of FOX transcription factor–binding

sites in a large proportion of WT1-bound regions, thus supporting the model of a coordinated action of these two transcription factors.

Although WT1(−KTS) isoforms are well-established transcriptional regulators, the role of WT1(+KTS) is less clear. Previous studies have shown that it can bind to RNA

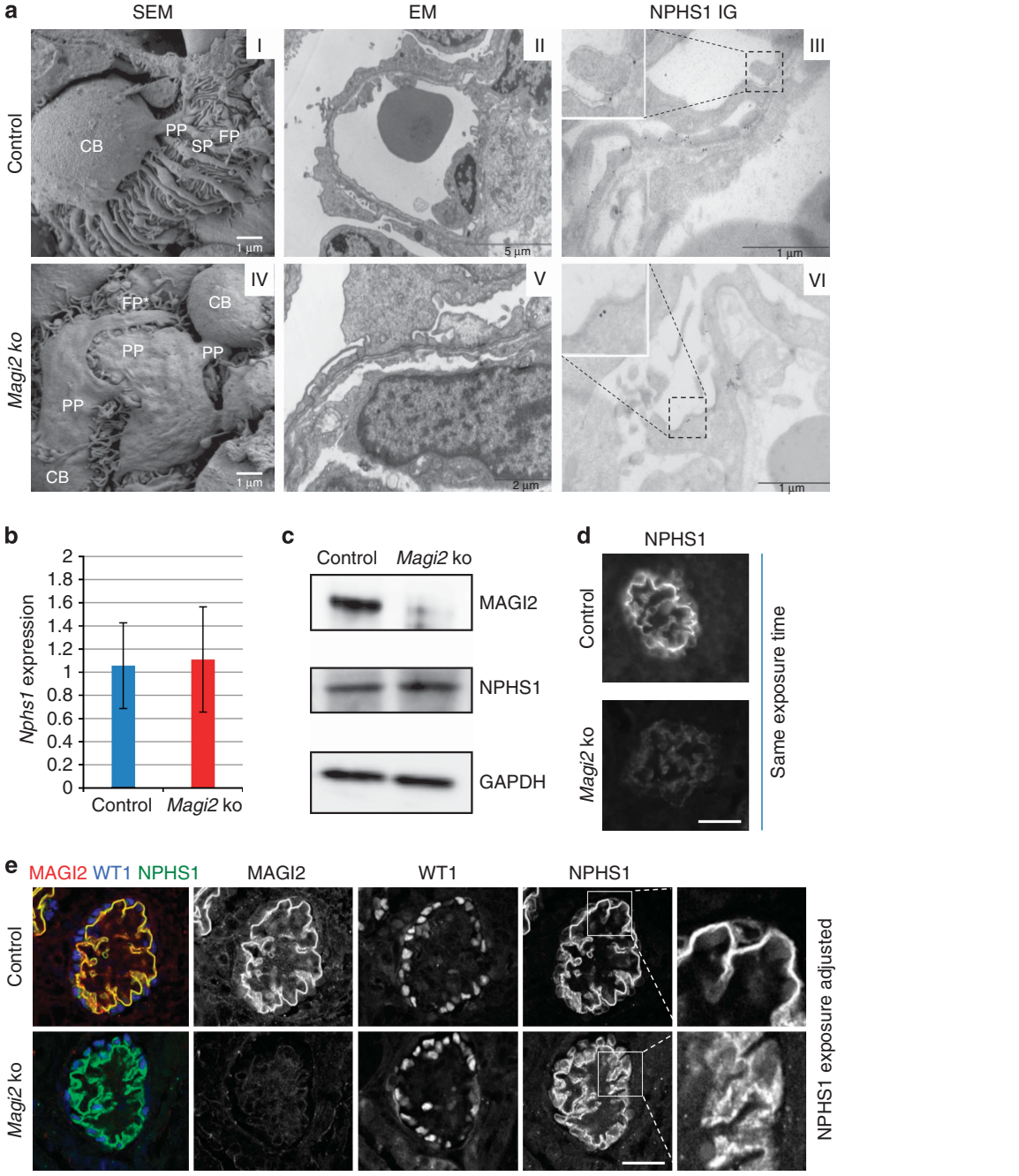

Figure 4 | *Magi2*α knockout (KO) mice fail to develop glomerular foot processes and a proper slit diaphragm. (**a**) Scanning electron micrographs (SEMs; I and IV) show an aberrant morphology of *Magi2*α KO podocytes that develop primary processes, but lack highly developed network of foot processes, replaced instead by filopodia-like structures. CB, cell body; FP, foot process; FP*, abnormally developed foot processes; PP, primary process; SP, secondary process. Transmitted electron microscopy (II and V) shows the morphology of these abnormal foot processes that lack a proper slit diaphragm and display a thicker basal membrane. Nephrin Immunogold labeling (III and VI) confirms the presence of NPHS1 protein in the mutants, but the localization is mostly intracytoplasmic compared with the extracellular localization at the slit diaphragm level of the control (higher magnification inserts). (**b**) Quantitative reverse transcription–PCR (RT-PCR) analysis performed on P0 kidneys indicates no significant change in *Nphs1* expression between control and *Magi2*α KO mice. (**c**) This observation is confirmed by western blot analysis showing comparable abundance of NPHS1 protein between control and *Magi2*α mutant mice. GAPDH, glyceraldehyde 3-phosphate dehydrogenase. (**d**) Immunofluorescence staining of NPHS1 reveals a markedly reduced signal in *Magi2* knockout mice, when compared with controls at the same exposure time. (**e**) Immunofluorescence staining confirmed the absence of MAGI2 protein in *Magi2*α mutant animals. After prolonged exposure, NPHS1 in knockout animals signal reveals punctuated and cytoplasmic staining (most right panels). Scale bar = 25 µm.

and copurify with splicing factors, thus suggesting a potential role in alternative splicing. Our exon array analyses with RNA isolated from WT1(+KTS) knockout mice could not confirm such a role. Although at present we cannot rule out technical reasons for the failure to detect differentially spliced genes, our data would rather support the regulation at the

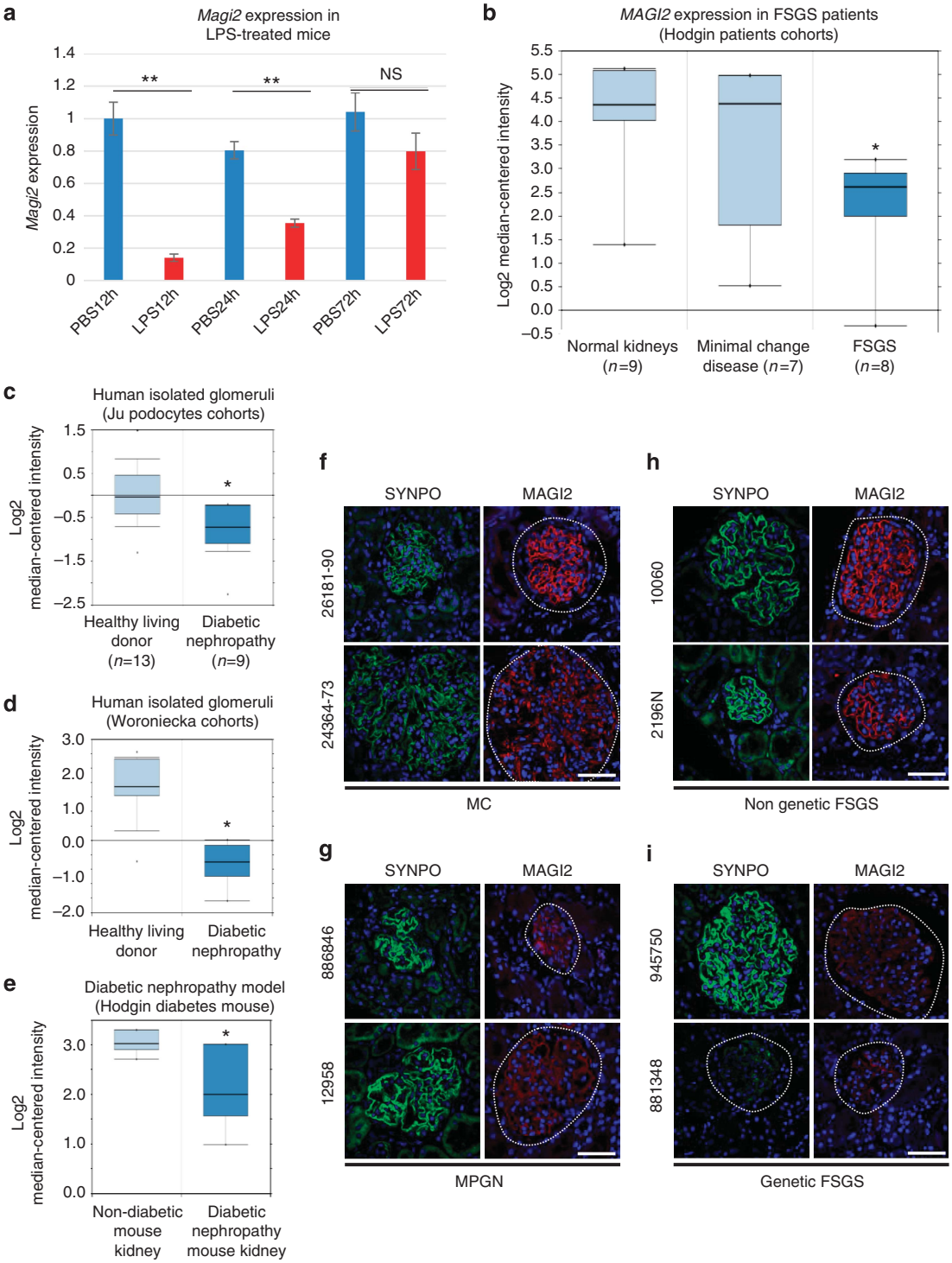

Figure 5 | Reduced *Magi2* expression is associated with glomerular diseases. (**a**) Lipopolysaccharide (LPS)-treated mice show a marked, but transient, reduction in *Magi2* expression ($n = 3$, $^{**}P < 0.01$). PBS, phosphate-buffered saline. (**b–e**) Analysis of the Nephromine database (www.nephromine.org) revealed reduced expression in patients suffering from (**b**) focal segmental glomerulosclerosis (FSGS), (**c**, **d**) diabetic nephropathy, and (**e**) in a mouse model of diabetic nephropathy ($^{*}P < 0.05$). (**f–i**) Immunofluorescence staining of SYNPO and MAGI2 in human patients affected by (**f**) minimal change (MC) disease, (**g**) membranous proliferative glomerulonephritis (MPGN), (**h**) nongenetic FSGS, and (**i**) genetic FSGS (*945750*: *NPHS2*; *881348*: *COQ2* mutations). Dotted lines outline glomeruli. Scale bar = 50 µm.

transcriptional level. Indeed, a high proportion of genes downregulated in *Wt1(+KTS)* mutant animals also have proximal WT1-binding sites. Although WT1(+KTS) by itself does not bind well to DNA, regulation through interacting cofactors has been demonstrated in other systems. For example, WT1(+KTS) appears to interact with GATA4 to direct the expression of the sex determining gene *Sry*.[34]

Deletion of *Wt1(+KTS)* also resulted in increased expression of a set of genes. However, as only a very small proportion of these genes are associated with WT1 peaks, a direct suppression by WT1 seems unlikely. Instead, we believe the induction of these genes to be a secondary event caused by abnormal foot process formation and the associated cellular stress. Consistent with this hypothesis, GOrilla analysis revealed enrichment of the categories immune response/chemokine activity and axon guidance/neuron projection. The program of foot process formation requires marked changes in cytoskeletal organization that overlap with that required for neuronal projections.[14] We speculate that the increased expression of these genes is caused by a persistent attempt of podocytes to form the required projections. In contrast, genes that fall into the category 'chemokine activity' and more generally 'immune response' may be induced in response to glomerular damage caused by abnormal podocyte differentiation.

The kidney phenotype of *Magi2* knockout mice has been recently reported, with the two models showing defects of distinct severity. Although deletion of exon 4 resulted in progressive loss of glomerular function,[26] truncation of *Magi2* after exon 5 (mutation cassette inserted within exon 6) led to a complete absence of the slit diaphragm.[25] Our own study clarifies and extends these observations. First, the very similar phenotype of our mice to that seen by Ihara *et al.*[25] confirms the essential role of MAGI2 in slit diaphragm assembly and suggests that the allele by Balbas *et al.*[26] represents a hypomorph. In this respect, it is interesting to note that exon skipping of exon 4 (the exon mutated in Balbas *et al.*[26]) would not result in truncation of the protein, but the deletion of 71 amino acids and we can speculate that such a protein would retain some functionality. Second, the knockout allele examined in this study leaves MAGI2β and MAGI2γ intact, and we can conclude that MAGI2α is the predominant and essential isoform in glomerular podocytes. Third, we report that although nephrin expression persists at the RNA level, immunodetection with antibodies was severely affected. Regulation of nephrin protein translation by MAGI2, as hypothesized by Ihara *et al.*,[25] can be ruled out, as nephrin protein levels on a denaturing western blot were unchanged. We therefore propose that MAGI2 is required for the assembly of the slit diaphragm and/or unfolding of the nephrin protein that renders the epitope accessible for antibody binding. Of note, Dai *et al.*[35] reported a similar redistribution of nephrin in podocytes lacking the integrin-linked kinase ILK, and this might suggest common molecular mechanisms in these two mutants. Alternatively, MAGI2 function may have a more general role in Rho-dependent actin rearrangement, a function it seems to hold within neuronal cells.[22]

Although *Magi2* clearly has an essential function in slit diaphragm assembly, expression in WT1(+KTS) mutant animals was only 2.3-fold reduced. As heterozygous *Magi2*α mutants do not show a clear kidney phenotype, it is unlikely that the reduction of *Magi2* is solely responsible for the Frasier phenotype. Future analysis will therefore have to concentrate on some of the other genes deregulated in the Frasier mutant. However, the marked changes of MAGI2 expression observed in *Nephromine* analysis and the confirmation of severe loss of MAGI2 protein in some cases of glomerular disease may suggest that mutations in this gene may be causative in some human patients. Of note, *MAGI2* has also been identified as a gene in close proximity to single-nucleotide polymorphisms associated with compromised renal function assessed by estimated glomerular filtration rate,[36] thus further supporting a potential involvement of this gene in glomerular disease in humans.

MATERIALS AND METHODS

Animals

All animal work was conducted according to national and international guidelines and has been approved by the local ethics committee (NCE/2011-19). *WT1* splice–specific[11] and *Magi2*α mutant mice[22] were maintained on a mixed genetic background (C57Bl6 crossed with B6D2F1) and *genotyped* using genomic DNA extracted from *biopsies* (Supplementary Table S1 online).

Bioinformatic analysis

Genes associated with WT1-bound peaks (IDR <0.1)[13] were compared with cell type–specific gene lists obtained from the GUDMAP website (www.gudmap.org)[14,37] using the Venny online tool (http://bioinfogp.cnb.csic.es/tools/venny/). For peak visualization (Figure 2c), the UCSC (University of California, Santa Cruz) genome browser was used in combination with the track hub http://129.94.136.7/tracks/WT1_NCOMMS_13_12838B/hub.txt. Motif discovery was performed using the MEME suite and compared with databases using TOMTOM and AME. Scripts are available on request.

Array analyses

Glomeruli from E18.5 *Wt1(+KTS)*$^{-/-}$ and wild-type control embryos were isolated as previously described.[38] RNA was extracted using Trizol, processed and hybridized on the Mouse Exon V1 Array (Affymetrix, High Wycombe, UK). Arrays were quantile-normalized and low-level transcripts (<50) were removed. Analysis on alternative splicing events was performed using the two-way analysis of variance approach of the Partek Genomic Suite version 6.4 (Partek, St Louis, MO). Differential expression of summarized gene level expression was calculated using the f-test statistic, followed by false discovery rate multiple testing correction. List comparisons (Figures 2 and 3) with cell type–specific gene lists[14,37,39] were prepared using the Venny online tool (http://bioinfogp.cnb.csic.es/tools/venny/). All array data are available on Gene Expression Omnibus browser, GEO access number: GSE67313 (http://www.ncbi.nlm.nih.gov/geo/query/acc.cgi?acc=GSE67313).

Human studies

Kidney biopsy specimens from patients with glomerulopathies were obtained from anonymized kidney biopsy materials kindly provided by participants of the PodoNet Registry (PMID: 25635037).

LPS analysis

The 4–6-week-old 129 female Swiss mice were treated with LPS essentially as previously described,[27] except that the dosage was 10 μg LPS per g body weight (1 mg/ml LPS in phosphate-buffered saline). Control animals were injected with 10 μl phosphate-buffered saline per g body weight. At the designated time, glomeruli were isolated according to Takemoto *et al.*[40] and RNA was extracted with Trizol.

ChIP and quantitative real-time PCR quantifications

Kidneys were dissected from E18.5 mouse embryos and diced in ice-cold Hanks' buffered saline solution. ChIP was performed essentially as previously described,[13] and quantitative real-time PCR was carried out using Light Cycler TaqMan Master Kit (Roche Diagnostic, Meylan, France) and normalized on input material (specific primers and probes listed in the Supplementary Table S2 online).

Magi2 promoter study

The promoter region ranging from −1800 to −1 of the upstream region of murine *Magi2* was amplified by PCR. Two different lengths of the promoter, including, respectively, two binding sites (1.8 kb) or only one (0.4 kb), were cloned into a pGL2 luciferase reporter plasmid. U2OS cells were cotransfected (X-tremeGENE HP DNA Transfection Reagent; Roche) with the above reporter plasmids, a CMV-βGal vector for standardization, and an pcDNA3 expression vector encoding either WT1(−KTS), WT1(+KTS), or the empty vector. After 48 h, cells were lysed and the luciferase activity was assessed using the Luciferase assay kit (Promega) and normalized to β-galactosidase activity (Promega assay, Lyon, France).

For detailed protocols on proteins/RNA extraction and analysis, electron microscopy, and immuno/hystological analysis, please refer to Supplementary Materials and Methods online.[41,42] Details of the antibodies used are listed in Supplementary Table S3 online.

DISCLOSURE

All the authors declared no competing interests.

ACKNOWLEDGMENTS

We thank members of the animal facility at the iBV for technical assistance and Norbert Hübner and Sabine Schmidt (MDC Berlin) for help with Exon-Array analysis. We are grateful to Christoph Englert (Jena) for the kind gift of the WT1-C8 antibody. This work was supported by grants from the FRM (Fondation pour la Recherche Médicale, DEQ20090515425), ANR (ANR-08-GENOPAT-017 and ANR-11-LABX-0028-01), Fondation du Rein and ARC (SL22020605297), E-Rare (German Ministry of Education and Research), and the EU 7th framework Programme (EURenOmics, grant 2012-305608); STB was financed by the Association Française contre les myopathies (AFM).

SUPPLEMENTARY MATERIAL

Figure S1. Distinct effects on podocyte marker gene expression in splice-specific WT1 mutants.
Figure S2. Consensus sequences identified in podocyte-specific promoter regions bound by WT1.
Figure S3. Array quality control.
Figure S4. Expression analysis of deregulated genes in Wt1(+KTS)-/- glomeruli.
Figure S5. Magi2 promoter study.
Figure S6. Deletion of exon1 completely abolishes Magi2 expression in mouse kidneys.
Figure S7. Characterization of Magi2 mutants.
Figure S8. Absence of Magi2 does not affect the fenestration of glomerular endothelial cells layer.
Figure S9. Nephromine analysis reveals loss of MAGI2 expression in several glomerular diseases.
Supplementary Data S1. Analysis of ChIP-Seq data in relation to podocyte-specific gene expression.
Supplementary Data S2. Exon-Array analysis.
Supplementary Data S3. GOrilla analysis.
Supplementary Table S1. List of primers for genotyping.
Supplementary Table S2. List of primers for qPCR.
Supplementary Table S3. List of antibodies.
Supplementary material is linked to the online version of the paper at http://www.nature.com/ki

REFERENCES

1. Welsh GI, Saleem MA. Nephrin-signature molecule of the glomerular podocyte? *J Pathol* 2010; **220**: 328–337.
2. Lehtonen S, Ryan JJ, Kudlicka K *et al.* Cell junction-associated proteins IQGAP1, MAGI-2, CASK, spectrins, and alpha-actinin are components of the nephrin multiprotein complex. *Proc Natl Acad Sci USA* 2005; **102**: 9814–9819.
3. Rigothier C, Auguste P, Welsh GI *et al.* IQGAP1 interacts with components of the slit diaphragm complex in podocytes and is involved in podocyte migration and permeability in vitro. *PLoS One* 2012; **7**: e37695.
4. Hohenstein P, Hastie ND. The many facets of the Wilms' tumour gene, WT1. *Hum Mol Genet* 2006; **15**(Spec No 2): R196–R201.
5. Davies RC, Calvio C, Bratt E *et al.* WT1 interacts with the splicing factor U2AF65 in an isoform-dependent manner and can be incorporated into spliceosomes. *Genes Dev* 1998; **12**: 3217–3225.
6. Larsson SH, Charlieu JP, Miyagawa K *et al.* Subnuclear localization of WT1 in splicing or transcription factor domains is regulated by alternative splicing. *Cell* 1995; **81**: 391–401.
7. Pelletier J, Bruening W, Kashtan CE *et al.* Germline mutations in the Wilms' tumor suppressor gene are associated with abnormal urogenital development in Denys-Drash syndrome. *Cell* 1991; **67**: 437–447.
8. Barbaux S, Niaudet P, Gubler MC *et al.* Donor splice-site mutations in WT1 are responsible for Frasier syndrome. *Nat Genet* 1997; **17**: 467–470.
9. Klamt B, Koziell A, Poulat F *et al.* Frasier syndrome is caused by defective alternative splicing of WT1 leading to an altered ratio of WT1 +/-KTS splice isoforms. *Hum Mol Genet* 1998; **7**: 709–714.
10. Bruening W, Bardeesy N, Silverman BL *et al.* Germline intronic and exonic mutations in the Wilms' tumour gene (WT1) affecting urogenital development. *Nat Genet* 1992; **1**: 144–148.
11. Hammes A, Guo JK, Lutsch G *et al.* Two splice variants of the Wilms' tumor 1 gene have distinct functions during sex determination and nephron formation. *Cell* 2001; **106**: 319–329.
12. Wagner N, Wagner KD, Xing Y *et al.* The major podocyte protein nephrin is transcriptionally activated by the Wilms' tumor suppressor WT1. *J Am Soc Nephrol* 2004; **15**: 3044–3051.
13. Motamedi FJ, Badro DA, Clarkson M *et al.* WT1 controls antagonistic FGF and BMP-pSMAD pathways in early renal progenitors. *Nat Commun* 2014; **5**: 4444.
14. Brunskill EW, Georgas K, Rumballe B *et al.* Defining the molecular character of the developing and adult kidney podocyte. *PLoS One* 2011; **6**: e24640.
15. Moriguchi T, Hamada M, Morito N *et al.* MafB is essential for renal development and F4/80 expression in macrophages. *Mol Cell Biol* 2006; **26**: 5715–5727.
16. Kestila M, Lenkkeri U, Mannikko M *et al.* Positionally cloned gene for a novel glomerular protein–nephrin–is mutated in congenital nephrotic syndrome. *Mol Cell* 1998; **1**: 575–582.
17. Boute N, Gribouval O, Roselli S *et al.* NPHS2, encoding the glomerular protein podocin, is mutated in autosomal recessive steroid-resistant nephrotic syndrome [published erratum appears in Nat Genet 2000;25 (1):125]. *Nat Genet* 2000; **24**: 349–354.
18. McLeay RC, Bailey TL. Motif Enrichment Analysis: a unified framework and an evaluation on ChIP data. *BMC Bioinformatics* 2010; **11**: 165.
19. Eden E, Navon R, Steinfeld I *et al.* GOrilla: a tool for discovery and visualization of enriched GO terms in ranked gene lists. *BMC Bioinformatics* 2009; **10**: 48.
20. Hirao K, Hata Y, Ide N *et al.* A novel multiple PDZ domain-containing molecule interacting with N-methyl-D-aspartate receptors and neuronal cell adhesion proteins. *J Biol Chem* 1998; **273**: 21105–21110.
21. Ihara KI, Nishimura T, Fukuda T *et al.* Generation of Venus reporter knock-in mice revealed MAGI-2 expression patterns in adult mice. *Gene Expr Patterns* 2012; **12**: 95–101.

22. Iida J, Ishizaki H, Okamoto-Tanaka M *et al.* Synaptic scaffolding molecule alpha is a scaffold to mediate N-methyl-D-aspartate receptor-dependent RhoA activation in dendrites. *Mol Cell Biol* 2007; **27**: 4388–4405.
23. Hirao K, Hata Y, Yao I *et al.* Three isoforms of synaptic scaffolding molecule and their characterization. Multimerization between the isoforms and their interaction with N-methyl-D-aspartate receptors and SAP90/PSD-95-associated protein. *J Biol Chem* 2000; **275**: 2966–2972.
24. Essafi A, Webb A, Berry RL, Slight J *et al.* A wt1-controlled chromatin switching mechanism underpins tissue-specific wnt4 activation and repression. *Dev Cell* 2011; **21**: 559–574.
25. Ihara KI, Asanuma K, Fukuda T *et al.* MAGI-2 is critical for the formation and maintenance of the glomerular filtration barrier in mouse kidney. *Am J Pathol* 2014; **184**: 2699–2708.
26. Balbas MD, Burgess MR, Murali R *et al.* MAGI-2 scaffold protein is critical for kidney barrier function. *Proc Natl Acad Sci USA* 2014; **111**: 14876–14881.
27. Reiser J, von Gersdorff G, Loos M *et al.* Induction of B7-1 in podocytes is associated with nephrotic syndrome. *J Clin Invest* 2004; **113**: 1390–1397.
28. Guo G, Morrison DJ, Licht JD, Quaggin SE. WT1 activates a glomerular-specific enhancer identified from the human nephrin gene. *J Am Soc Nephrol* 2004; **15**: 2851–2856.
29. Ristola M, Arpiainen S, Saleem MA *et al.* Transcription of nephrin-Neph3 gene pair is synergistically activated by WT1 and NF-kappaB and silenced by DNA methylation. *Nephrol Dial Transplant* 2012; **27**: 1737–1745.
30. Schumacher VA, Schlotzer-Schrehardt U, Karumanchi SA *et al.* WT1-dependent sulfatase expression maintains the normal glomerular filtration barrier. *J Am Soc Nephrol* 2011; **22**: 1286–1296.
31. Ratelade J, Arrondel C, Hamard G *et al.* A murine model of Denys-Drash syndrome reveals novel transcriptional targets of WT1 in podocytes. *Hum Mol Genet* 2010; **19**: 1–15.
32. Gebeshuber CA, Kornauth C, Dong L *et al.* Focal segmental glomerulosclerosis is induced by microRNA-193a and its downregulation of WT1. *Nat Med* 2013; **19**: 481–487.
33. O'Brien LL, Grimaldi M, Kostun Z *et al.* Wt1a, Foxc1a, and the Notch mediator Rbpj physically interact and regulate the formation of podocytes in zebrafish. *Dev Biol* 2011; **358**: 318–330.
34. Miyamoto Y, Taniguchi H, Hamel F *et al.* A GATA4/WT1 cooperation regulates transcription of genes required for mammalian sex determination and differentiation. *BMC Mol Biol* 2008; **9**: 44.
35. Dai C, Stolz DB, Bastacky SI *et al.* Essential role of integrin-linked kinase in podocyte biology: Bridging the integrin and slit diaphragm signaling. *J Am Soc Nephrol* 2006; **17**: 2164–2175.
36. Kottgen A, Pattaro C, Boger CA *et al.* New loci associated with kidney function and chronic kidney disease. *Nat Genet* 2010; **42**: 376–384.
37. Brunskill EW, Sequeira-Lopez ML, Pentz ES *et al.* Genes that confer the identity of the renin cell. *J Am Soc Nephrol* 2011; **22**: 2213–2225.
38. Cui S, Li C, Ema M *et al.* Rapid isolation of glomeruli coupled with gene expression profiling identifies downstream targets in Pod1 knockout mice. *J Am Soc Nephrol* 2005; **16**: 3247–3255.
39. Harding SD, Armit C, Armstrong J *et al.* The GUDMAP database–an online resource for genitourinary research. *Development* 2011; **138**: 2845–2853.
40. Takemoto M, Asker N, Gerhardt H *et al.* A new method for large scale isolation of kidney glomeruli from mice. *Am J Pathol* 2002; **161**: 799–805.
41. Courtney M, Gjernes E, Druelle N *et al.* The inactivation of Arx in pancreatic alpha-cells triggers their neogenesis and conversion into functional beta-like cells. *PLoS Genet* 2013; **9**: e1003934.
42. Lefebvre J, Muharram G, Leroy C *et al.* Caspase-generated fragment of the Met receptor favors apoptosis via the intrinsic pathway independently of its tyrosine kinase activity. *Cell Death Dis* 2013; **4**: e871.
43. Holt DS, Botto M, Bygrave AE *et al.* Targeted deletion of the CD59 gene causes spontaneous intravascular hemolysis and hemoglobinuria. *Blood* 2001; **98**: 442–449.
44. Yabuta Y, Ohta H, Abe T *et al.* TDRD5 is required for retrotransposon silencing, chromatoid body assembly, and spermiogenesis in mice. *J Cell Biol* 2011; **192**: 781–795.
45. Matsuyama S, Aihara K, Nishino N *et al.* Enhanced long-term potentiation in vivo in dentate gyrus of NELL2-deficient mice. *Neuroreport* 2004; **15**: 417–420.
46. Gu C, Yoshida Y, Livet J *et al.* Semaphorin 3E and plexin-D1 control vascular pattern independently of neuropilins. *Science* 2005; **307**: 265–268.
47. Schluter OM, Schmitz F, Jahn R *et al.* A complete genetic analysis of neuronal Rab3 function. *J Neurosci* 2004; **24**: 6629–6637.
48. Sosinowski T, Killeen N, Weiss A. The Src-like adaptor protein downregulates the T cell receptor on CD4+CD8+ thymocytes and regulates positive selection. *Immunity* 2001; **15**: 457–466.
49. Cosgrove D, Meehan DT, Grunkemeyer JA *et al.* Collagen COL4A3 knockout: a mouse model for autosomal Alport syndrome. *Genes Dev* 1996; **10**: 2981–2992.
50. Roselli S, Heidet L, Sich M *et al.* Early glomerular filtration defect and severe renal disease in podocin-deficient mice. *Mol Cell Biol* 2004; **24**: 550–560.
51. Wharram BL, Goyal M, Gillespie PJ *et al.* Altered podocyte structure in GLEPP1 (Ptpro)-deficient mice associated with hypertension and low glomerular filtration rate. *J Clin Invest* 2000; **106**: 1281–1290.
52. George M, Rainey MA, Naramura M *et al.* Renal thrombotic microangiopathy in mice with combined deletion of endocytic recycling regulators EHD3 and EHD4. *PLoS One* 2011; **6**: e17838.
53. Douarre C, Sourbier C, Dalla Rosa I *et al.* Mitochondrial topoisomerase I is critical for mitochondrial integrity and cellular energy metabolism. *PLoS One* 2012; **7**: e41094.
54. Graham JR, Chamberland A, Lin Q *et al.* Serine protease HTRA1 antagonizes transforming growth factor-beta signaling by cleaving its receptors and loss of HTRA1 in vivo enhances bone formation. *PLoS One* 2013; **8**: e74094.
55. Shi ZZ, Han B, Habib GM *et al.* Disruption of gamma-glutamyl leukotrienase results in disruption of leukotriene D(4) synthesis in vivo and attenuation of the acute inflammatory response. *Mol Cell Biol* 2001; **21**: 5389–5395.
56. Lavery GG, Walker EA, Draper N *et al.* Hexose-6-phosphate dehydrogenase knock-out mice lack 11 beta-hydroxysteroid dehydrogenase type 1-mediated glucocorticoid generation. *J Biol Chem* 2006; **281**: 6546–6551.
57. Sun X, Funk CD, Deng C *et al.* Role of decay-accelerating factor in regulating complement activation on the erythrocyte surface as revealed by gene targeting. *Proc Natl Acad Sci USA* 1999; **96**: 628–633.